

STRUCTURE OF HEN EGG-WHITE LYSOZYME

A Three-dimensional Fourier Synthesis at 2 Å Resolution

By DR. C. C. F. BLAKE, DR. D. F. KOENIG*, DR. G. A. MAIR, DR. A. C. T. NORTH†, DR. D. C. PHILLIPS†, and DR. V. R. SARMA

Davy Faraday Research Laboratory, Royal Institution, 21 Albemarle Street, London, W.1

THE X-ray analysis of the structure of hen egg-white lysozyme¹ (*N*-acetylmuramide glycanohydrolase, *EC* 3.2.1.17), which was initiated in this Laboratory in 1960 by Dr. R. J. Poljak, has now produced a Fourier map of the electron density distribution at 2 Å resolution in which the structure of the molecule can be clearly seen.

Comparison of this map with the primary structure, determined by Jollès *et al.*^{2,3}, by Canfield^{4,5} and in part by Brown⁶, has made possible the location of each of the 129 amino-acid residues of which the molecule is composed, many of which, including the four disulphide bridges, can be identified unambiguously in the X-ray image. The arrangement of groups in the molecule is very complicated, and many interactions between them will be revealed only by detailed analysis of the map. This preliminary account of the work is intended, therefore, to indicate the quality of the results, and to show the general structure of the molecule. Further work which is described in the following article⁷ has also revealed the location of a site at which competitive inhibitor molecules are bound in the crystal structure so that it is possible, even at this stage, to identify amino-acid residues which may be involved in the binding of substrates.

X-ray Methods

Crystals of hen egg-white lysozyme chloride grown at pH 4.7 (ref. 8) are tetragonal with unit cell dimensions, $a = b = 79.1$, $c = 37.9$ Å, and space group $P4_12_12$ or $P4_32_12$ (ref. 9). Each unit cell contains eight lysozyme molecules (one per asymmetric unit), molecular weight about 14,600, together with 1 M sodium chloride solution which constitutes about 33.5 per cent of the weight of the crystal¹⁰.

A preliminary investigation¹¹, in which the method of isomorphous replacement was used, showed that the space group is in fact $P4_22_12$ and made possible a calculation of the electron density distribution at 6 Å resolution.

In the extension of this analysis to higher resolution it has been necessary to find new and better isomorphous heavy-atom derivatives. Those originally used contained: (1) mercuri-iodide ions; (2) chloropalladite ions; and (3) *ortho*-mercuri hydroxytoluene *para*-sulphonic acid (MHTS) and of these only the MHTS derivative was found to be suitable for work at higher resolution. An extensive search, using methods already described¹¹, revealed, however, that derivatives containing (4) $UO_2F_5^{2-}$ (ref. 12); and (5) an ion derived from $UO_2(NO_3)_2$, probably $UO_2(OH)_n^{(n-2)-}$, were very suitable for this purpose. In addition derivatives including (6) *para*-chloromercuri benzene sulphonic acid (PCMBs) and (7) $PtCl_6^{2-}$ (ref. 13) were found to be satisfactory for use at low resolution. All these derivatives except (1) and (2) were used in a re-examination of the structure at 6 Å. The necessary diffraction measurements were made with the Hilger and Watts, Ltd., linear diffractometer¹⁴ adapted to measure three reflexions at a time^{15,16} and the data were processed and the other calculations made on the Elliott 803 B computer at the Royal Institution. The phases were calculated by the phase probability method¹⁷, adapted

to make proper allowance for anomalous scattering of the copper $K\alpha$ X-rays by the various heavy atoms¹⁸. The availability of uranium derivatives was particularly fortunate in that the anomalous scattering effect is large for uranium and indeed a particular search was made for them with that in mind. The mean figure of merit obtained in these calculations was 0.97 as compared with the 0.86 obtained before, and the greater part of this improvement has been shown to arise from the improved treatment of anomalous scattering rather than from the inclusion of additional heavy-atom derivatives.

Fig. 1 shows a model of the electron-density distribution at 6 Å resolution obtained in this new work. The outline of the molecule is certainly clearer in the new map than in the old, and within the molecule there is improved continuity suggesting the course of a folded polypeptide chain; but the two maps are, in fact, very similar (root mean square difference in electron density 0.12 eÅ⁻³) and it remains impossible to determine the structure from them in any detail. Nevertheless a tentative general interpretation was possible. The model can be divided roughly into two parts; on the left-hand side of Fig. 1 the density has the appearance of a single chain without cross-connections while to the right the arrangement appears to be much more complex. In general agreement with the picture, the primary structure, shown in Fig. 2, includes some relatively long lengths of polypeptide chain free from cross-connections together with a region in which two disulphide bridges and two proline residues are close together.

2 Å Resolution

In preparation for the high-resolution investigation, the various heavy-atom derivatives were investigated in the centro-symmetric $hk0$ and $h0l$ projections at 3 and 2 Å resolution. Comparison of the various sign predic-

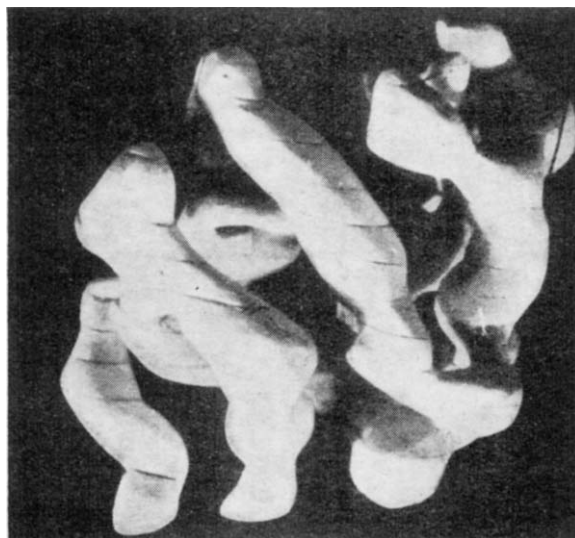


Fig. 1. Solid model of the lysozyme electron-density greater than about 0.5 electrons/Å³ at 6 Å resolution

* Present address: Brookhaven National Laboratory, Upton, Long Island, New York.

† Medical Research Council External Staff.

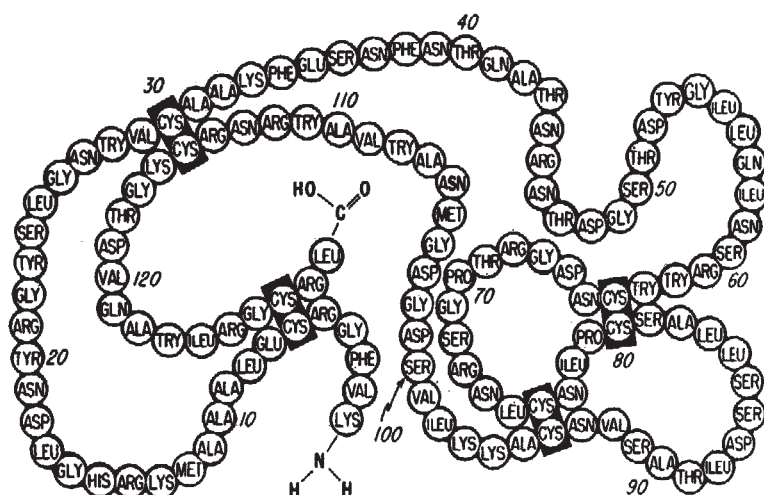


Fig. 2. Sequence of amino-acid residues in hen egg-white lysozyme reproduced from Canfield and Liu (ref. 5)

tions and examination of the radial distributions of the intensity differences¹⁹ showed that only derivatives (3), (4) and (5) were suitable for high-resolution work. Accordingly 2 Å data were collected from the native crystals and for crystals containing these heavy atoms. The same experimental methods were used; but in order to minimize the effects of irradiation damage each crystal was exposed for only 20 h or less to the β -filtered X-ray beam from a copper tube operated at 40 kV, 20 m.amp. About 16 crystals were used to obtain each set of measurements which included generous overlaps for scaling²⁰ and separate measurement of the reflexions in the Bijvoet pairs hkl and $\bar{h}\bar{k}\bar{l}$. Semi-empirical corrections were made for absorption²¹. The data-processing system was designed at every stage to detect errors and to avoid their introduction and to eliminate any need for comprehensive manual checking.

The complete set of 2 Å data comprises some 9,040 reflexions of which 1,640 are centric, a property of this space group which greatly facilitates the determination and refinement of the heavy-atom parameters. The main heavy-atom positions were all found from $(\Delta F)^2$ maps in projection, and subsidiary sites were found from ΔF maps in two and three dimensions when preliminary signs and phases had been found. The best parameters were determined by the use of the quasi-three-dimensional set of centric reflexions, $hk0$, $k0l$, hhl , $0kl$, in an adaptation of Hart's method²². The final parameters are shown in Table 1. The large proportion of centric reflexions also made possible an examination of the variation in apparent occupancy with scattering angle, thus revealing the shape of the appropriate scattering factor curve for each heavy-atom. These curves agree well with those expected for a heavy central atom surrounded by a shell of light atoms replacing a sphere of uniform electron density.

The temperature factors shown in Table 1 most deserve comment. Those obtained for the most important sites (of which there are no more than two for any derivative)

Table 1. HEAVY-ATOM PARAMETERS

Site	X	Y	Z	O	B	F	N	R
MHTS	I 0.2068	0.6138	0.0507	39.2	17.8	58	1247	0.60
	II 0.2415	0.6308	0.9326	8.8	14.9			
UO ₃ F ₂	I 0.1783	0.5840	0.7204	55.5	21.0	74	1277	0.52
	II 0.0074	0.8976	0.4650	29.8	24.2			
UO ₃ (OH) ₂	I 0.0961	0.8988	0.4664	47.1	19.2	80	1140	0.57
	II 0.1898	0.5901	0.7168	42.1	124.8			
	III 0.0446	0.7266	0.5515	9.0	190.2			
	IV 0.0860	0.8976	0.4866	11.4	68.4			
	V 0.2024	0.6888	0.6781	28.6	42.8			

O, Occupancy of heavy-atom site—electrons; B, isotropic temperature factor constant—Å²; F, root mean square difference between observed and calculated heavy-atom changes for centric reflexions—electrons; N, number of centric reflexions in the range $0.01 < \sin^2\theta < 0.15$ used in refinement; R, reliability index for observed and calculated heavy-atom changes of centric reflexions.

are all comparable with the overall value for the protein crystals themselves. The very large values obtained for other sites of (5) show that these sites are of little importance at high angles and may not represent true sites of heavy-atom attachment. The minor site of (3) MHTS is clearly the SO₃⁻ group of this molecule: it occupies the same position as the equivalent group in the not strictly isomorphous PCMBs derivative²³.

The refinement programme gave the root mean square 'lack of closure' errors required in the isomorphous phase determination¹⁷ that are shown in Table 1. Analysis of the agreement obtained between measurements of symmetry equivalent reflexions gave the corresponding values required for the anomalous-scattering phase determination¹⁸. These were found to vary as a function of $\sin\theta$ having the values $19 + 455 \sin^2\theta/\lambda^2$ for derivatives (3) and (4) and $26.5 + 485 \sin^2\theta/\lambda^2$ for derivative (5).

The phases of the 9,040 reflexions were calculated on the Elliott 803 B computer and had a mean figure of merit of 0.60. The variation with angle was very similar to that obtained in the comparable analysis of sperm-whale myoglobin²⁴; the mean value fell to 0.38 at the 2 Å limit. The 'best'¹⁷ electron-density distribution, unsharpened, was calculated from these phases and 'figures-of-merit' on the University of London Atlas computer. The density was calculated at 1/120ths of the cell edge along a and b and 1/60ths along c , and was tabulated in a form suitable for immediate contouring to a scale of 0.75 in. \equiv 1 Å. The Elliott 803 B computer was used to generate that part of the map which was expected, from the 6 Å resolution work, to include one molecule, from the arbitrary asymmetric unit calculated by Atlas. The absolute scale of the measurements is known only roughly (from statistical arguments and reasonable occupancies for the heavy-atoms) and the map was contoured at estimated 0.25 eÅ⁻³ intervals.

The Fourier Map

The electron-density corresponding to a single molecule extends over the full length of the c -axis of the unit cell and in the other axial directions lies within the ranges $-\frac{1}{2} < x < +\frac{1}{2}$, $0 < Y < \frac{1}{2}$. The contour map was plotted on 60 sections of constant Z so as to extend safely beyond these ranges of X and Y . Two separate blocks of ten sections each, which are representative of the whole map, are shown in Figs. 3 and 4. No $F(000)$ term was included in the Fourier synthesis, so that density values are all relative to the average crystal density. Only contours of higher than average density are shown in the maps, but there are no patches of high negative density even at the heavy atom positions, and it is immediately apparent that the general background is satisfactorily uniform. In regions which must be occupied by water and salt⁹, such as those near the two-fold rotation axes, there are many small peaks, which are consistent with some degree of order in the liquid of crystallization. Within the molecular boundary the density indicates clearly the course of the polypeptide chain and the nature of many side-chains.

At this resolution atoms are not expected to appear in the image as separate peaks of electron density, but groups of atoms connected only by ionic or van der Waals' interactions or by hydrogen bonds are expected to be resolved. It is satisfactory therefore to find a continuous ribbon of high density with characteristic features at regular intervals to represent the main polypeptide chain with its carbonyl groups and with side-chains protruding

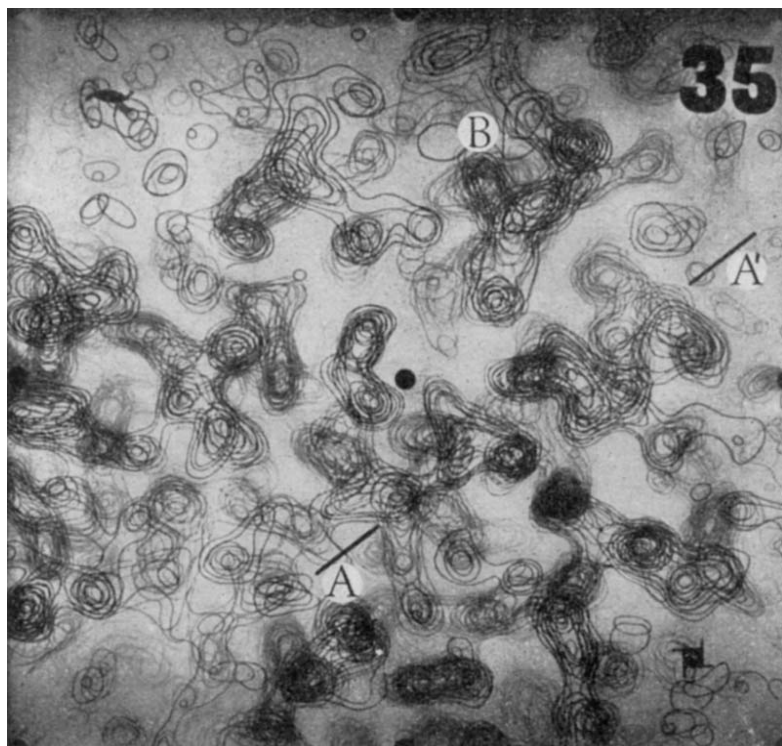


Fig. 3. Sections $Z=35-41/60$ of the 2 Å resolution electron density map. Contours at intervals of 0.25 eÅ^{-3} . AA' shows the course of a length of α -helix lying in the plane of the sections. B indicates a length of helix more nearly normal to the sections

from it. In some regions the conformation of the main chain is clearly α -helical. For example, Fig. 3 includes the density corresponding to two lengths of α -helix, one of which runs approximately parallel to the sections (AA') while the other is more nearly perpendicular to the sections (B). Inspection of the density in comparison with models shows immediately that the helices are right-handed running towards the terminal amino end of the polypeptide chain in the direction AA' and at B down into the map.

It is in such helical regions that the side-chains are most easily identified. Thus the peak of high density a little below the helix AA' and connected back to it clearly represents a disulphide bridge between the helix and more extended chain near the bottom of the picture. To the left of the disulphide bridge, density characteristic of another side-chain, a phenylalanine, can be seen emerging from the helix at an α -carbon position four residues removed from the cystine towards the terminal carboxyl end of the chain. This observation, when combined with the sequence of Fig. 2, immediately identifies the disulphide bridge as that between residues 30 and 115 and was, in fact, the starting-point of a detailed correlation between map and sequence. The helix at B corresponds to a part of the chain nearer the terminal amino end and has features clearly consistent with the sequence Arg-Lys-Met-Ala-Ala-Ala of residues 14-9.

In the non-helical regions, the courses of the main chain and the side-chains are rather less easily recognized by mere inspection of the map. Nevertheless, no real difficulty was encountered in following the main chain and nowhere did the density corresponding to it fall to the general background-level. As in

the corresponding study of myoglobin²⁵, however, it was often simpler to recognize the density corresponding to particular well-marked side-chains than to follow the main-chain density directly. Some of these clearly identifiable side-chains in a non-helical region are shown in Fig. 4. They include most prominently the indole rings of tryptophan residues 28, 108 and 111, and the sulphur atom of methionine 105 which come together with tyrosine 23 in this part of the structure to form a curiously regular hydrophobic box.

Of course, not all the residues are as clearly recognizable as this; but using the criteria formulated in the examination of myoglobin²⁵ it is possible to identify many of them with considerable confidence. Nevertheless, the existence of almost complete knowledge of the primary structure has been of enormous value, and no attempt was made to analyse the X-ray image without recourse to it. No disagreements with the chemical information were obvious at this stage of analysis except in those few small regions in which the chemical studies^{2,4} do not agree. These are discussed here.

General Description of the Molecule

The molecule is roughly ellipsoidal with dimensions about $45 \times 30 \times 30 \text{ Å}$. The general arrangement of the polypeptide chain is indicated in the schematic diagram of Fig. 5. It is clearly even more complicated than that of myoglobin, and a comprehensive description cannot yet be given. Some important features, however, are immediately apparent. First, the α -helical content is relatively low. Detailed in-

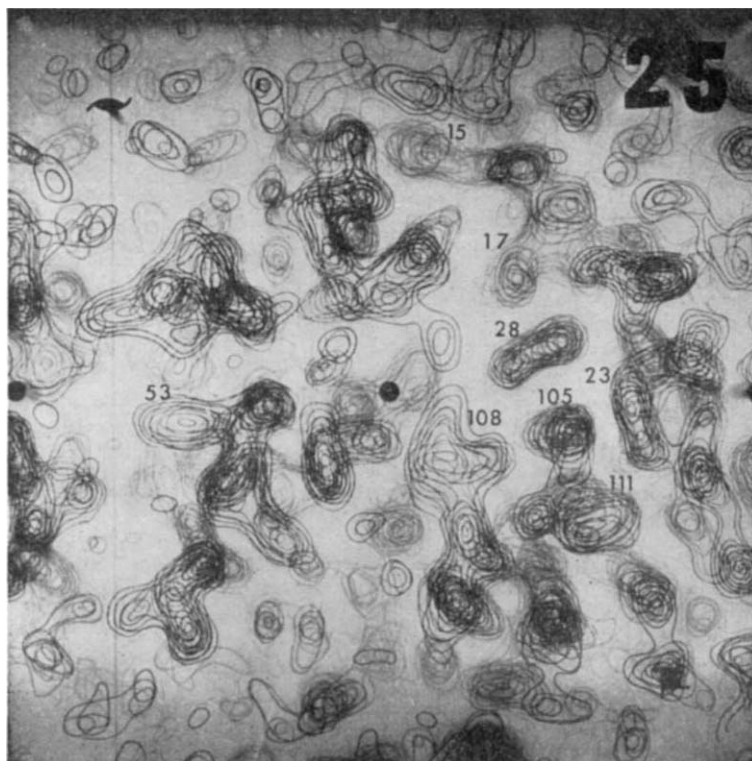


Fig. 4. Sections $Z=25-34/60$ of the 2 Å resolution electron density map. The densities corresponding to a number of amino-acid side-chains are numbered in accordance with Fig. 2

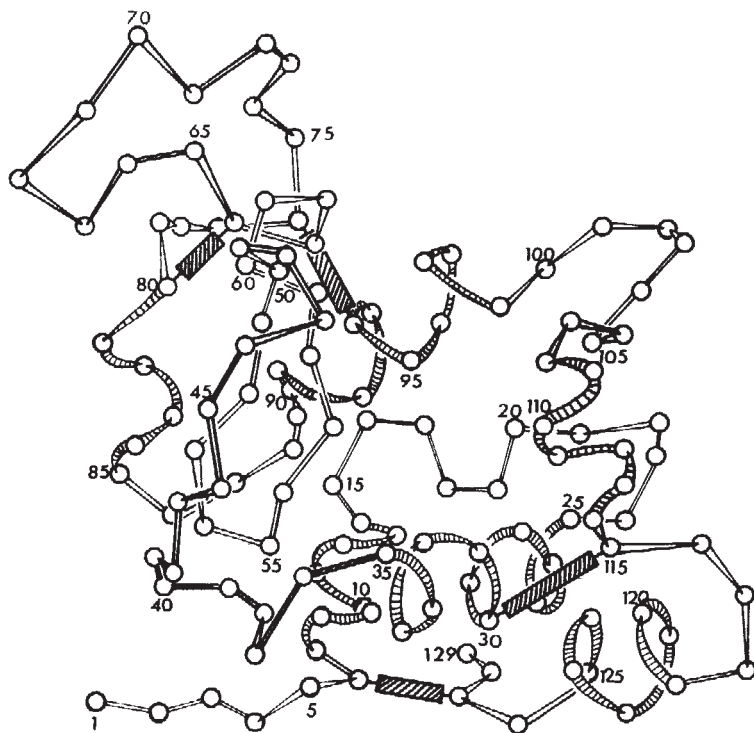


Fig. 5. Schematic drawing of the main chain conformation (by W. L. Bragg)

vestigations of the helical parameters have not yet been made, but about six lengths of helix have been recognized, some of them very short, as indicated in Figs. 5 and 6. If a residue is regarded as being in a helix if one or other of its possible hydrogen bonds is properly made, then about 55 of the 129 residues appear at this stage to be included in helices. This suggests a maximum helix content of about 42 per cent, in fair agreement with the predictions of optical rotatory dispersion^{26,27}.

The remainder of the molecule is less easily described, the folding of residues 35-80 being particularly complex. In this region three lengths of chain are roughly anti-parallel, two of them, residues 41-54, forming a nearly closed loop. Nearby are the two closely related disulphide bridges connected by short lengths of chain which include the proline residues (70 and 79).

The disulphide bridges each have a helix on at least one side, although the half-cystine is generally the last helical residue or at least in the last turn of its helix. Only one bridge, 30-115, has a helix on both sides and 115 is a terminal residue.

The inside and outside of the molecule are less easily defined than they are for myoglobin, in which the interior of the molecule consists almost exclusively of hydrophobic side-chains²⁸. The lysozyme molecule appears to have a hydrophobic spine consisting mainly of the six tryptophan side-chains and including the hydrophobic box already described (Fig. 4). Three of these tryptophan side-chains, 62, 63 and 123, protrude, however, beyond the molecular boundary and there are in addition a number of strongly hydrophobic side-chains clearly on the molecular surface (for example, Val 2, Phe 3, Phe 34, Leu 17).

On the other hand, the parts of the molecule most shielded from contact with surrounding liquid appear to include

Ser(91) and Gln(57). In addition, residue 58, which may be asparagine², can be regarded as internal. All the lysine and arginine side-chains are external.

Comparison with Low Resolution Results

It is interesting to compare this molecule with the model obtained at 6 Å resolution. The boundary of the molecule was correctly chosen in the revised 6 Å work (Fig. 1) and was incorrect only in minor details in the earlier investigation¹¹. Furthermore, the very general interpretation was correct in that the complex folding indicated by the right-hand part of Fig. 1 does indeed include the two disulphide bridges 64-80 and 76-94. On the other hand, it is somewhat surprising to discover that the 6 Å maps contain no significant indications of the positions of three of the disulphide bridges, possibly because they lie in diffraction minima associated with neighbouring helices. Clearly it is very unlikely indeed that the 6 Å model could have been interpreted correctly in detail, even in the light of the primary structure, and this is true also of a model at 5 Å resolution which is not described here.

Comparison with Chemical Data

The independent investigations of the primary structure^{2,4,5} now agree in all but a few details on the sequence of amino-acid residues in the lysozyme molecule. Two of the remaining doubts⁹ are concerned with the distinction between aspartic acid and asparagine, which are not readily distinguishable by the X-ray method. The other three difficulties, which are more serious, can be resolved to some extent by examination of the present map.

Thus, residues 92 and 93 are included in a length of helix and their side-chains have strongly contrasted appearances. That of 92 is clearly forked close to the helix and is surrounded by a clear region of low electron density, while the side-chain of residue 93 is longer and approaches much more nearly to neighbouring density. It is probable, therefore, that the sequence 92-93 is valine-asparagine⁴ rather than asparagine-valine². In the second case, the side-chains associated with residues 40-42, which are in a non-helical region, appear to be much more consistent

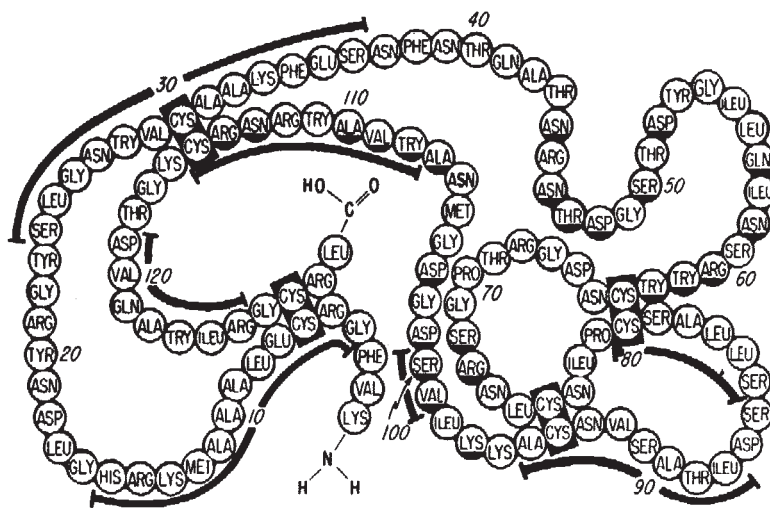


Fig. 6. Primary structure (ref. 5) showing (continuous line) the residues found in α -helical conformation and those in the apparent binding site (underlined)

(by similar arguments) with the sequence Thr-Gln-Ala⁴ than with Gln-Ala-Thr². The third ambiguity, between isoleucine and asparagine in positions 58 and 59, has already been referred to. In this case the differences between the two densities are less clear, but on balance that associated with residue 58 seems more consistent with asparagine² than with isoleucine⁴ even though this residue can be regarded as being inside the molecule. Its environs include the disulphide bridge 76-94 and Leu 83, but also serine 91, and there is an unexplained neighbouring patch of density which could represent an included water molecule. It is hoped that the detailed analysis of side-chain interactions which is now in progress will resolve this uncertainty.

In addition to the primary structure there are, of course, very many chemical data on the physical and chemical properties of lysozyme which cannot be discussed here, but which are expected to be interpretable eventually in terms of the detailed structure. Something must now be said, however, about amino-acid residues probably concerned in the enzymatic activity, a subject on which there is so far rather little definite chemical evidence.

Inhibitor Binding Site

The following article describes the location at low resolution of the site of attachment of *N*-acetyl-glucosamine and its dimer, chitobiose, both of which molecules act as competitive inhibitors of lysozyme. They attach themselves, at least in this crystal structure, in a cleft in the surface of the molecule which runs nearly vertically down the middle of Fig. 5 and which can be seen clearly in the low-resolution model (Fig. 1, ref. 7). The amino-acid residues bounding this portion of the molecular surface come from various parts of the polypeptide chain and are indicated in Fig. 6. Clearly, further examination is required to establish whether this site represents the binding site of substrate molecules, but for the present it seems a reasonable hypothesis that it does so and that the properties of these residues may well repay detailed investigation. In accordance with chemical evidence²⁹⁻³², they include three tryptophans, now shown to be 62, 63 and 108, but not the single histidine which is located on the opposite side of the molecule.

We thank Sir Lawrence Bragg, who drew the diagram of Fig. 5, and Prof. R. King for their advice, and the Managers of the Royal Institution for their support; the Director of the London University Computer Unit for facilities on *Atlas*; and Mrs. R. Arthanari, Mrs. W. Browne, Mrs. S. J. Cole, Mrs. J. A. Conisbee, Miss M. Hibbs, Mrs. K. Sarma and Messrs. A. R. Knott, S. B. Morris and J. E. T. Thirkell for their assistance. We also thank the Medical Research Council and the U.S. National Institutes of Health for financial support.

- ¹ Fleming, A., *Proc. Roy. Soc.*, B, **93**, 306 (1922).
- ² Jollès, J., Jauregui-Adell, J., and Jollès, P., *Biochim. Biophys. Acta*, **78**, 68 (1963).
- ³ Jollès, P., Jauregui-Adell, J., and Jollès, J., *C.R. Acad. Sci., Paris*, **258**, 3926 (1964).
- ⁴ Canfield, R. E., *J. Biol. Chem.*, **238**, 2698 (1963).
- ⁵ Canfield, R. E., and Liu, A. K., *J. Biol. Chem.* (in the press).
- ⁶ Brown, J. R., *Biochem. J.*, **92**, 13P (1964).
- ⁷ Johnson, L. N., and Phillips, D. C. (following article).
- ⁸ Alderton, G., and Fevold, J., *J. Biol. Chem.*, **164**, 1 (1946).
- ⁹ Palmer, K. J., Ballantyre, M., and Galvin, J. A., *J. Amer. Chem. Soc.*, **70**, 906 (1948).
- ¹⁰ Steinrauf, L. K., *Acta Cryst.*, **12**, 77 (1959).
- ¹¹ Blake, C. C. F., Fenn, R. H., North, A. C. T., Phillips, D. C., and Poljak, R. J., *Nature*, **196**, 1173 (1962).
- ¹² Holmes, K. C., and Leberman, R., *J. Mol. Biol.*, **6**, 439 (1963).
- ¹³ Poljak, R. J., *J. Mol. Biol.*, **6**, 244 (1963).
- ¹⁴ Arndt, U. W., and Phillips, D. C., *Acta Cryst.*, **14**, 807 (1961).
- ¹⁵ Phillips, D. C., *J. Sci. Instrum.*, **41**, 123 (1964).
- ¹⁶ Arndt, U. W., North, A. C. T., and Phillips, D. C., *J. Sci. Instrum.*, **41**, 421 (1964).
- ¹⁷ Blow, D. M., and Crick, F. H. C., *Acta Cryst.*, **12**, 794 (1959).
- ¹⁸ North, A. C. T., *Acta Cryst.*, **13**, 212 (1965).
- ¹⁹ Crick, F. H. C., and Magdoff, B. S., *Acta Cryst.*, **9**, 901 (1956).
- ²⁰ Hamilton, W. C., Rollett, J. S., and Sparks, R. A., *Acta Cryst.*, **18**, 129 (1965).
- ²¹ North, A. C. T., Phillips, D. C., and Mathews, F. S. (in preparation).
- ²² Hart, R. G., *Acta Cryst.*, **14**, 1188 (1961).
- ²³ Blake, C. C. F., Fenn, R. H., and Phillips, D. C. (in preparation).
- ²⁴ Kendrew, J. C., Dickerson, R. E., Strandberg, B. E., Hart, R. G., Davies, D. R., Phillips, D. C., and Shore, V. C., *Nature*, **185**, 422 (1960).
- ²⁵ Kendrew, J. C., Watson, H. C., Strandberg, B. E., Dickerson, R. E., Phillips, D. C., and Shore, V. C., *Nature*, **190**, 663 (1961).
- ²⁶ Urnes, P., and Doty, P., *Adv. Prot. Chem.*, **16**, 401 (1961).
- ²⁷ Hamaguchi, K., and Imahori, K., *J. Biochem. (Japan)*, **55**, 388 (1964).
- ²⁸ Kendrew, J. C., *Brookhaven Symp. Quant. Biol.*, **15**, 216 (1962).
- ²⁹ Kravchenko, N. A., Kleopina, G. V., and Kaverzneva, E. D., *Biochim. Biophys. Acta*, **92**, 412 (1964).
- ³⁰ Bernier, I., and Jollès, P., *C.R. Acad. Sci., Paris*, **253**, 745 (1961).
- ³¹ Ramachandran, L. K., and Rao, G. J. S., *Biochim. Biophys. Acta*, **59**, 507 (1962).
- ³² Hartdegen, F. J., and Rupley, J. A., *Biochim. Biophys. Acta*, **92**, 625 (1964).

STRUCTURE OF SOME CRYSTALLINE LYSOZYME-INHIBITOR COMPLEXES DETERMINED BY X-RAY ANALYSIS AT 6 Å RESOLUTION

By Miss LOUISE N. JOHNSON and Dr. D. C. PHILLIPS*

Davy Faraday Research Laboratory, Royal Institution, 21 Albemarle Street, London, W.1

A RECENT investigation of the azide derivative of sperm-whale myoglobin¹ has shown that the interactions of proteins with small molecules can be examined in crystals when the phases of reflexions from isomorphous unsubstituted-protein crystals are known. The difference Fourier method is used in which the changes in structure amplitude caused by the introduction of the small molecule are combined with the known phases to give a map showing the change in electron density. The work on myoglobin¹ was done at 2 Å resolution; but we have now shown that interesting results can be obtained by this method at 6 Å resolution even when the substituted molecules comprise only light atoms. The method depends on the existence of precise phase information for the protein crystals, information which is now available for lysozyme², and by its means we have been able to investi-

gate the structural relationship between lysozyme and a number of compounds which are related to the substrate of the enzyme and which act as competitive inhibitors of its action. In this way we have been able to locate a part of the molecule which may be responsible for its enzymatic activity.

Lysozyme has a $\beta(1-4)$ glucosaminidase activity with the ability to hydrolyse a mucopolysaccharide component of some bacterial cell walls releasing *N*-acetyl amino sugars derived from glucosamine and muramic acid³. The proposed structure of a tetrasaccharide⁴ isolated from the cell wall of *Micrococcus lysodeikticus*, which is made up of alternate *N*-acetylglycosamine and *N*-acetyl muramic acid units, is shown in Fig. 1 in which the bond probably hydrolysed by lysozyme is indicated by an arrow. Lysozyme will also hydrolyse chitin⁵, the (1-4) linked linear chain polymer of *N*-acetylglucosamine, and Wenzel *et al.*⁶ have shown that lysozyme will promote the cleavage of the trimer, tri-*N*-acetyl chitotriose,

* Medical Research Council External Staff.